Identification of X-ray Beam Instability Sources for a MX Beamline at the ESRF

M. Lesourd, R.B.G. Ravelli*, L. Zhang

European Synchrotron Radiation Facility – BP220 – 38043 Grenoble cedex - France
Phone: +33 4 76882306; Fax: +33 4 76882020
E-mail: lesourd@esrf.fr
**EMBL, Grenoble Outstation - BP156 – 30042 Grenoble cedex -France*

Abstract

The stability of the support of optical components, in particular monochromators and mirrors, is of crucial importance for most beamlines. A number of vibration analysis techniques, including modal testing, can be used to identify structural resonances. Due to the specific beamline configuration, only some of these vibrations affect the X-ray beam stability. A study of the correlation of the X-ray intensity with vibration measurements is necessary in order to highlight the most disturbing movements of the mechanical components of the beamline.
Such a study is presented for a tuneable Macromolecular Crystallography (MX) beamline at the European Synchrotron Radiation Facility (ESRF). The effect of pumps, monochromator crystal cooling and structural dynamic responses of relevant structures have been investigated. Significant improvements for the stability of this beamline were implemented as a result.

Keywords: Vibration, mechanical stability, beamline, X-ray intensity

1. Introduction

X-ray beam instabilities can originate from various sources that can arbitrarily be classified in three groups:

- Long term drift of the position of sensitive optics or mechanical supports. This can be due to thermal deformations for example.
- Mechanical vibrations of these components linked to the ground seismic activity (natural or “man made”). Actually, in the context of the ESRF, this means dynamic motions in the frequency range 1 to 100Hz. Outside this band it is generally accepted that the influence is not significant [1].
- Electron beam instabilities which, incidentally, result partly from the effect of the same perturbations applied to magnet-girder assemblies [2].

In this paper, we will focus on the second category. Mechanical stability of the beamline components is essential in order to maximise the quality of the data collected in a given experiment. Some optical devices are more prone to cause instabilities due to their inherent design. This is true for monochromators (Mono) and focussing mirrors. In most cases, the former uses a double reflection on two parallel crystals. This provides a quasi-fixed exit X-ray beam. However, the resultant beam energy is sensitive to relative motions of the 1st crystal with respect to the X-ray source, whereas differential movements between the two crystals can strongly affect the intensity. The focussing mirror reflects the X-rays impinging with grazing incidence on its generally slightly curved surface. With large lever arms, *i.e.* long distance between mirror and the experiment, mechanical vibrations can cause significant motion of the beam at the sample position.

We routinely characterise mechanical structures in terms of vibration amplitudes and frequency content using geophones or accelerometers. However, depending on the specific beamline configuration, not all vibrations will affect the X-ray beam stability. Therefore, a monitoring of the X-ray intensity in correlation with mechanical motions is required in order to pin point the most disturbing movements.

ID14-4 is a macromolecular crystallography beamline with a tuneable monochromator to allow for multiple anomalous diffraction (MAD) experiments. MAD exploits differences in the observed diffraction intensities caused by differential resonance effects of heavy atoms, such as Se, that are introduced in the macromolecular structure. Accurate measurement of these differences, that can be as small as 1-2%, allow crystallographers to solve the so-called phase problem, enabling them to calculate an experimental electron-density map, in which they can build their macromolecular model. The quality of the final electron-density map and thus, the amount of work it takes to build the model, is closely related to the quality of the diffraction data. The studies presented here have been done on ID14-4.

The following line of action was adopted:

- Study the behaviour of the relevant mechanical structures using Operating Response Measurement (ORM) and Operating Deflection Shape (ODS) analysis techniques.
- Identify vibration sources and their effects, *e.g.* vacuum pumps.
- Correlate X-ray intensity with vibration levels.
- Improve the mechanical design of the most sensitive components.

2. Instrumentation and Set-up

2.1 General Description

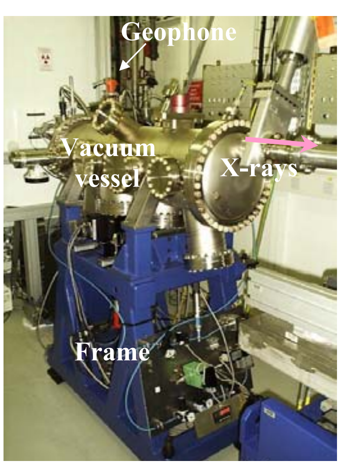

Fig. 1: Mirror downstream.

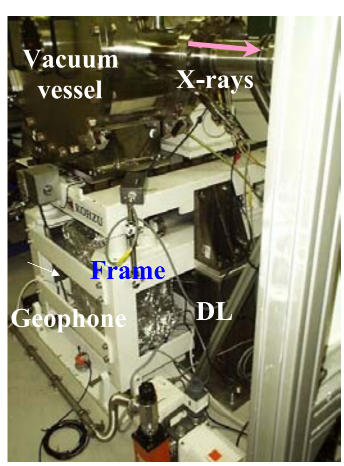

Fig. 2: Mono downstream.

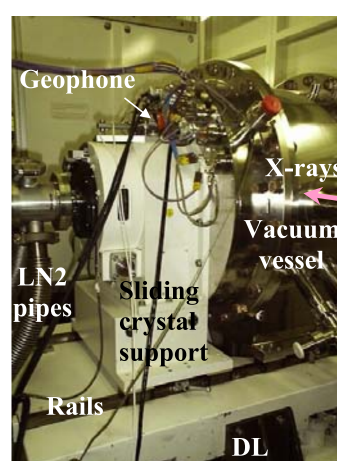

Fig. 3: Mono upstream.

Fig. 1, 2 and 3 show the mirror and Mono located in the ID14 optics hutch (OH2). The longitudinal (X) direction is along the X-ray path, while lateral (Y) is perpendicular.

The mirror vacuum vessel is mounted on a steel frame clamped to the concrete floor. The mirror itself is mechanically de-coupled from the vessel, its vertical position is controlled by three motorised jacks. The vertical focussing is regulated with a compressed air mechanical bender, whereas the mirror has a fixed curvature for horizontal focussing. The Kohzu Mono assembly has its frame resting on the floor with an intermediate steel plate allowing coarse horizontal alignment. The crystal support can be sled on guiding rails for changing from Si (111) to Si (311) crystals. The vacuum vessel is mounted on the same rails. In addition, liquid nitrogen (LN2) cooling is used to dissipate the high heat load on the crystals (Fig. 12). A Messer Griesheim (MG) cryogenic (cryo) system is operated outside OH2 that pumps LN2 to the crystal via pipes (visible on Fig. 3). In addition, several vacuum pumps are operated in OH2, including a turbo pump connected to the Mono vacuum vessel. The damping link (DL) is a structural modification of the structure carried out after the initial measurements (more details in section 6).

2.2 Sensors

For vibration level measurements, Mark Products L28 vertical and horizontal geophones were used. They provide a usable bandwidth of 4→100Hz and their relatively small size allows easy positioning on the structures. The X-ray beam intensity was monitored with a Hamamatsu photodiode placed in the beam either between the mono and mirror or close to the sample position in the experimental hutch (EH4). This device has an 18 x 18 mm2 sensitive area. No attempt was made to measure the position of the beam. The photodiode output was connected to a Keithley current to voltage amplifier.

These signals were digitised on a Siglab 20-42 spectrum analyser.

2.3 Operating Response Measurements (ORM)

For the ORM, vibration sensors were located on top of the mirror vessel, on the Mono crystal support and on the floor as seen on Fig. 1, 2 and 3. This allowed the extraction of some essential dynamic information about the structures: vibration amplitudes, peak frequencies and amplification factors with respect to floor. The ORM were repeated after suggested structural modifications were carried out on the Mono.

2.4 Operating Deflection Shapes (ODS) Analysis

An ODS analysis provides a view of the structure's motion at specified frequencies of interest. This is done in normal operating conditions, *i.e.* without additional excitation as required in the case of modal testing. Thus, as long as the vibration is stationary, randomly excited structures can be characterised. The excitation forces are not measured, only the observable responses define the deflection shapes. By measuring on a defined grid of locations on the Mono structure all referenced to a single data point, the phase relationship as well as the structural motion was determined [3].

3. Vibration Response of Mirror and Monochromator Assemblies

3.1 ORM for Mirror and Mono

Table 1 lists the peak to peak (d_{pp}) and rms (d_{rms}) displacements obtained at the relevant position on the structures. They are valid in the bandwidth (BW) 4→100Hz. In addition the amplification relative to floor motion (ratio) is also indicated. These are useful for comparison purposes since the vibration levels on the floor can vary with time and location.

Table 1: Peak to Peak Displacements in µm. Rms Values in Brackets

d_{pp} and d_{rms} in µm		Vertical (Z)	Longitudinal (X)	Lateral (Y)
Mirror	Floor	0.69 (0.09)	N/A	0.50 (0.09)
	Structure	0.72 (0.10)	N/A	0.86 (0.15)
	Ratio	**1.0**	N/A	**1.7**
Mono	Floor	0.65 (0.09)	0.23 (0.03)	0.28 (0.05)
	Structure	0.65 (0.07)	0.68 (0.11)	0.71 (0.12)
	Ratio	**1.0**	**3.0**	**2.5**

Note that, in the vertical direction, no major amplification with respect to floor occurs. Indeed the Power Spectral Density (PSD) (Fig. 4), reveal that the amplitudes are comparable on the floor and on the structures in the considered frequency range. In the lateral (Y) direction (Fig. 5), the PSD plots show large amplification with respect to floor motion on both structures. The Mono exhibits natural frequencies in the range 10 to 20Hz whereas the 1st mode on the mirror is around 20Hz [4]. Note that the contribution around 3Hz is linked to the ESRF site seismic response [1] and the 50Hz spike to electrical contamination of the measurement signals.

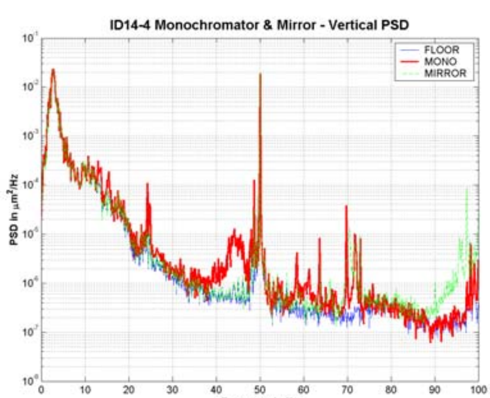

Fig. 4: Vertical PSD floor, mirror & Mono.

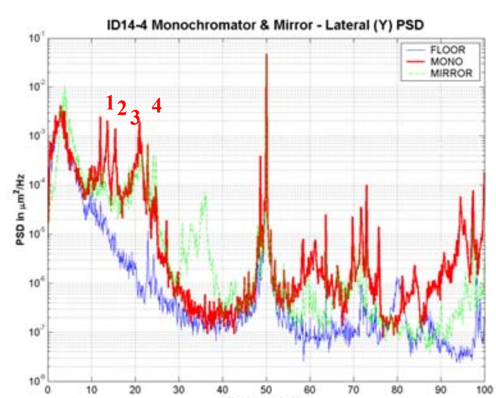

Fig. 5: Lateral (Y) PSD floor, mirror & Mono.

3.2 ODS for Mono

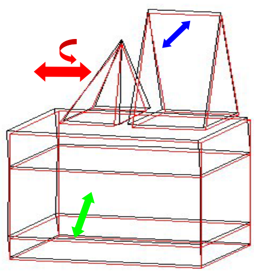

Fig. 6: Mode 1 at 12.75Hz.

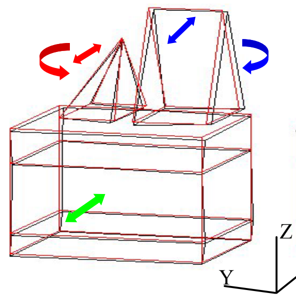

Fig. 7: Mode 2 at 14Hz.

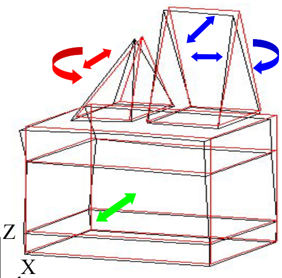

Fig. 8: Mode 3 at 15.5Hz.

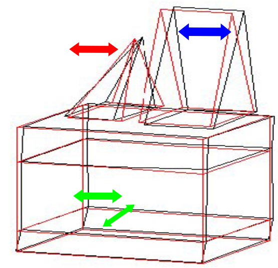

Fig. 9: Mode 4 at 21.9Hz.

Based on the results of the ORM displayed on Fig. 5, the first natural modes of the Mono structure were extracted after completion of the ODS analysis. Interestingly, these Mono vibration modes look very similar as far as deformed shapes are concerned (Figs. 6-9). They highlight the relative lack of stiffness of the frame and, more significantly, of the rail connecting the vacuum vessel and crystals to this frame. Movements have generally a component in the Y direction (⊥ to X-ray beam). The arrows indicate the direction and relative amplitudes at the given frequencies. Green, red and blue stand respectively for Mono frame, crystal support and vacuum vessel motions.

4. Identification of Vibration Sources

4.1 Mono Turbo Pump

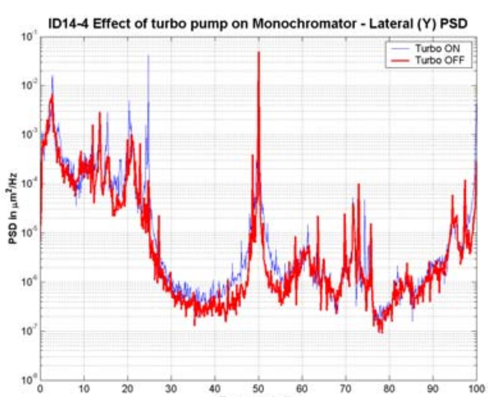

Fig. 10: Effect of the turbo pump.

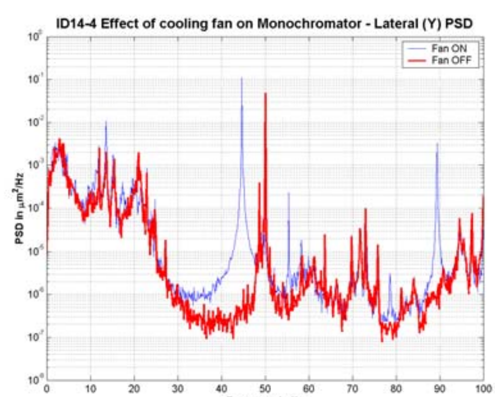

Fig. 11: Effect of the cooling fan on the turbo pump.

The Mono turbo pump is responsible for an excitation spectral line around 24.5Hz visible on Fig. 10. This is typical of an electrical rotating machinery, *i.e.*: the slip frequency for 4 poles motor with 50Hz power supply is of the order of 2% of the nominal frequency.

It is difficult to reduce this perturbation since the pump has to be close to the Mono vacuum vessel. However, due to improvements made on the vacuum of the Mono vessel, it is now possible to switch this turbo pump off during normal operation.

The effect of a fairly small cooling fan on the Mono turbo pump is also shown on Fig. 11. When this was in operation, the PSD recorded on the Mono clearly showed a spectral contribution at 44.6Hz and its 1st harmonic. In fact, as far as about 20m its influence could be measured on the floor and also on the neighbouring beamlines [5]. This was directly removed after identification!

4.2 LN2 Cooling System

The cooling circuit loop distributes LN2 both to the 1st and 2nd crystals. Originally, the latter was indirectly cooled, *i.e.* there was no circulation of cryo fluid close to the 2nd crystals. In order to improve the thermal stability of the 2nd pair of crystals of the monochromator, a LN2 cooling loop was implemented on these 2nd crystals. This was then upgraded to a more efficient version represented on Fig. 12.

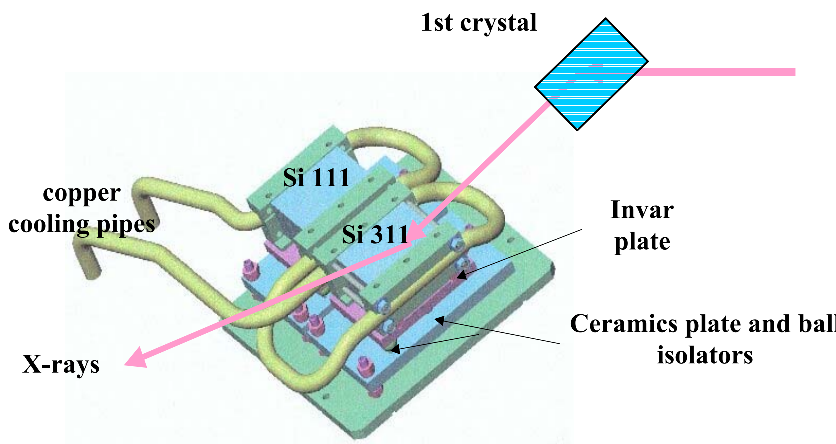

Fig. 12: 2nd crystal after modifications.

Measurements were made both with the 1st cooling version and the new design. A direct comparison on the X-ray beam stability was possible. We found optimum settings of the cryo pump speed that circulates the LN2 around the Mono crystals. The pump speed was linearly ramped up with time and both the X-ray beam intensity and the vibrations on the Mono were simultaneously monitored. Fig. 13, 14, 15 and 16 display the time-frequency plots of the results. The horizontal axis represents time (proportional to the cryo pump frequency) while the vertical axis is the frequency of the measured signals. Linear PSD spectra taken at low and high instability time slices are also shown.

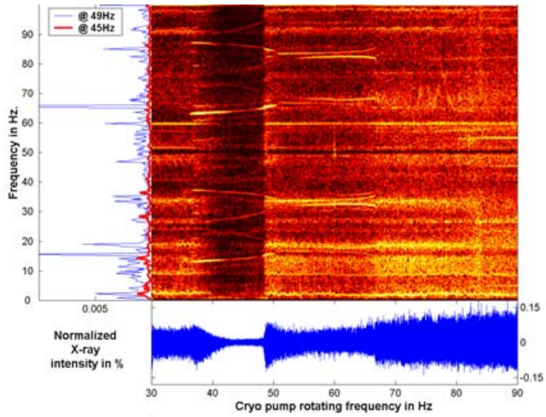

Fig. 13: X-ray intensity before modifications.

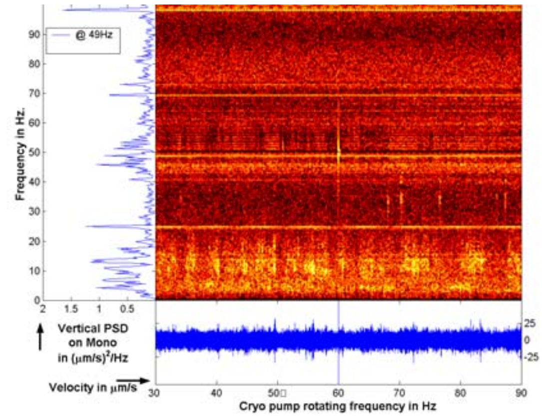

Fig. 14: Mono vibration before modifications.

Prior to the final upgrade of the 2nd crystal cooling, relatively quiet operating points could be reached at certain cryo pump regimes, while outside this narrow region, some sharp resonances were excited. At the highest flow rates, the observed broad band excitation points to possible turbulences occurring in the cooling circuit. Subsequently, the used operating frequency of the cryo pump was 45Hz. Note that no such effect was observed on the vibration signal on the Mono structure. Therefore, monitoring the X-ray intensity signal was essential in that respect. Indeed, no vibration sensor could be easily placed under vacuum condition directly on the crystal and in the beam, where the local excitation induced by LN2 flow could have been measurable.

The general behaviour changed greatly after a later upgrade in the 2nd crystal support that included the installation of a heavier motor. Note that the rotating frequencies now span from 35 to 65Hz. Also, the photodiode was located in EH4 instead of OH2. Therefore a direct quantification of the benefit of this new system cannot be achieved. However, the quieter regions seem to be wider than prior to modifications. Based on these observations, the beamline has been operated afterwards at a flow rate of 35Hz.

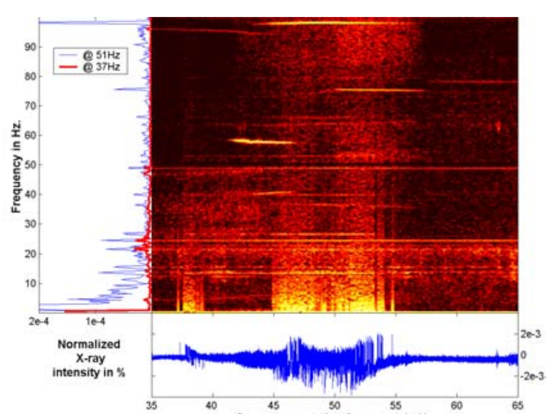

Fig. 15: X-ray intensity after modifications.

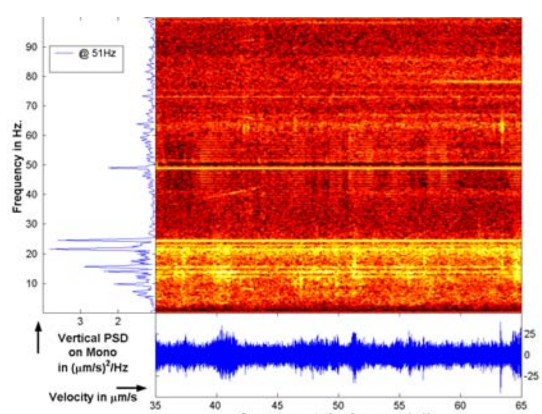

Fig. 16: Mono vibration after modifications.

5. Correlation X-ray Intensity versus Vibrations

A very good correlation was found between the X-ray intensity fluctuations and the lateral (Y) vibrations measured on the Mono sliding support. The agreement between both PSD spectra is particularly striking from 10 to 40Hz (Fig. 17). This is exactly where the lateral modes of the Mono lie. The coherence of the vibration and intensity is a mathematical representation of how good the correlation is. It takes the value 1 for well correlated down to zero for unrelated signals. The coherence is very close to 1 at the main frequency peaks (Fig. 18). The coherence was computed at two different cryo pump rotating frequencies in the "quiet" operating region at 35Hz, and also at 55Hz. Similar results were obtained.

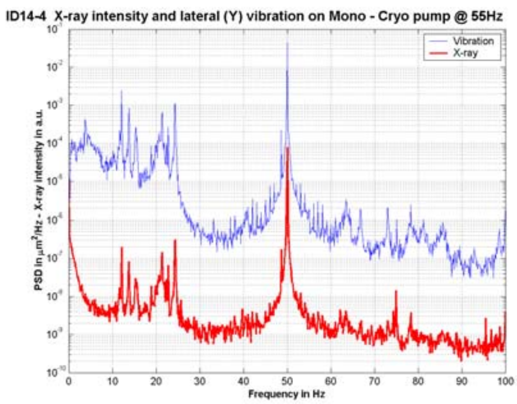

Fig. 17: Correlation X-ray intensity – Mono vibration

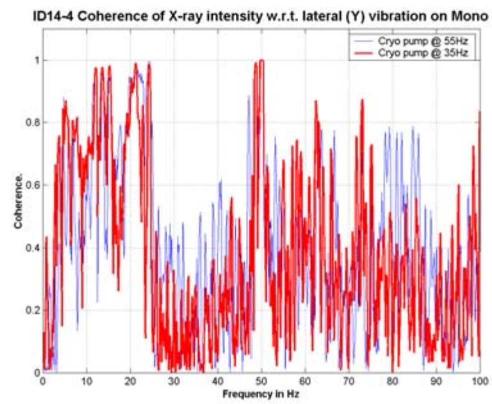

Fig. 18: Coherence of X-ray intensity with Mono vibration.

6. Mechanical improvements

The spectral amplitude of the floor excitation is decreasing with the square of the frequency [1], *i.e.*: there is about an order of magnitude more vibration level at 10Hz than at 30Hz. Therefore, one important factor to be considered when designing a structure is the frequencies of the first few natural vibration modes where amplifications with respect to the floor occur. In general terms, for a single degree of freedom the 1st resonance frequency can be expressed as:

$$f = \frac{1}{2\pi}\sqrt{K/M}$$

where f is the natural frequency, K the stiffness and M the mass. Hence, reducing the mass and / or rigidifying the structure will shift up the natural frequencies, away from the highest vibration components on the floor.

In view of the previous results, it was decided to improve the mechanical stability of the Mono assembly. Since substantially modifying the structure would have involved a lot of design work and a long intervention, it was decided to use external stiffening supports. This concept, the Damping Links (DL), has been developed and put in use at the ESRF for the magnet-girder assemblies [6]. It basically consists of one support firmly fixed to the floor, another one connected to the structure and an intermediate layer of viscoelastic material. The latter dissipates energy by shearing in the material, while the stiff steel fixtures add rigidity to the assembly. According to the ODS measured earlier, it seemed sensible to act mainly on horizontal motions. Therefore, the DL were positioned on both side of the Mono frame in order to act on lateral and longitudinal translations (Fig. 2).

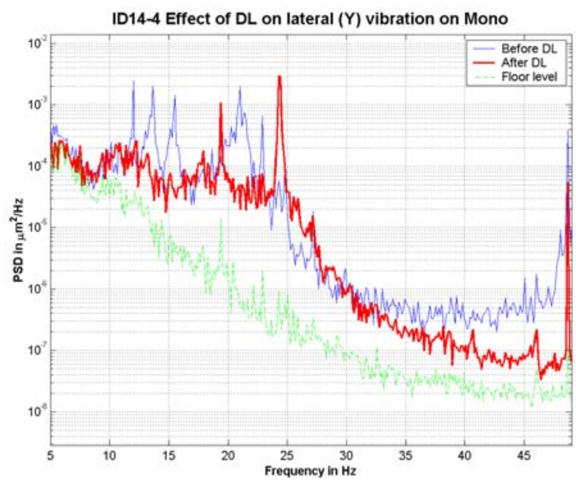

Fig. 19: Effect of the Damping Links

Although, the DL were not originally designed for this application, the PSD show very positive effects (Fig. 19). The four modes observed prior to installation have disappeared while a resonance at 24.8Hz has emerged. There is also a significant amplification of a spectral ray visible on the floor at 19Hz. It is possible that a turbo pump located in OH2 might excite or generate these frequency components. It is connected to the LN2 piping network and thus could transmit vibrations to the Mono. This will be further investigated. The values for d_{pp} before and after the installation of the damping links are given in Table 2.

Table 2: Mono Lateral Displacement Levels – Effect of Damping Links.
Peak to peak displacements in µm. Rms values in brackets.

d_{pp} and d_{rms} in µm	Before DL	After DL
Floor	0.28 (0.05)	0.28 (0.04)
Mono	0.71 (0.12)	0.58 (0.08)
Ratio w.r.t. floor	**2.5**	**2.1**

7. Conclusion

Vibration sources leading to X-ray instabilities have been identified on the ID14-4 MX beamline. As a result, steps were taken to reduce their influence. These included the selection of an appropriate cryo pump flow rate, phasing out turbo pump operation during experiments, and increasing the rigidity and damping of the Mono structure. This methodology proved very effective at highlighting the bottlenecks in the beamline design. Furthermore, these improvements could be implemented in a very efficient way, without having to interrupt the very tight and dense user program of the beamline. Future work will involve stiffening of the frame-crystal support mechanical interface on the Mono. Additionally, the correlation of the X-ray beam position with the vibrations on the mirror and, eventually the experimental table, will be subject to further studies.

8. Acknowledgements

The authors thank A. McCarthy, T. Mairs, S. McSweeney, W. Schmid, J. Surr and P. Theveneau for useful discussions and their help in providing technical information.

9. References

[1] L. Zhang, "Vibration at the ESRF," Vol. 2, EPAC96 (1996) 1359-1361.
[2] L. Zhang, L. Farvacque, J.M. Filhol, E. Plouviez, "E-Beam Stability Enhancement by Use of Damping Links for Magnet Girder Assemblies at the ESRF," PAC2001, Chicago, USA, (2001) 2620-2622.
[3] The STAR System™ user manual.
[4] M. Lesourd, "Modal analysis of the ID29 mirror assembly," ESRF internal report.
[5] M. Lesourd, "ID14 – Influence of local feedback and cell15 cryostat on the X-ray beam stability," ESRF internal report.
[6] L. Zhang, M. Lesourd, T. Lewis, "Vibration Damping Systems for Magnet Girder Assembly at the ESRF," PAC2001, Chicago, USA, (2001) 1465-1467.